HHS Public Access

Author manuscript

Cancer Res. Author manuscript; available in PMC 2022 April 06.

Published in final edited form as:

Cancer Res. 2020 August 01; 80(15): 3116–3129. doi:10.1158/0008-5472.CAN-19-3103.

Oncogenic Herpesvirus Engages Endothelial Transcription Factors SOX18 and PROX1 to Increase Viral Genome Copies and Virus Production

Silvia Gramolelli[1], **Endrit Elbasani**[1], **Krista Tuohinto**[1], **Veijo Nurminen**[1], **Thomas Günther**[2], **Riikka E. Kallinen**[1], **Seppo P. Kaijalainen**[1], **Raquel Diaz**[1], **Adam Grundhoff**[2], **Caj Haglund**[1,3], **Joseph M. Ziegelbauer**[4], **Teijo Pellinen**[5], **Mark Bower**[6], **Mathias Francois**[7], **Päivi M. Ojala**[1,8]

[1]Translational Cancer Medicine Research Program, Faculty of Medicine, University of Helsinki, Helsinki, Finland.

[2]Heinrich Pette Institute, Leibniz Institute for Experimental Virology, Hamburg, Germany.

[3]Department of Surgery, University of Helsinki and Helsinki University Hospital, Helsinki, Finland.

[4]HIV and AIDS Malignancy Branch, Center for Cancer Research, NCI, NIH, Bethesda, Maryland.

[5]Institute for Molecular Medicine Finland (FIMM), Helsinki Institute of Life Science (HiLIFE), University of Helsinki, Helsinki, Finland.

[6]National Centre for HIV Malignancy, Chelsea & Westminster Hospital, London, United Kingdom.

[7]The David Richmond Program for Cardio-Vascular Research: Gene Regulation and Editing, The Centenary Institute, The University of Sydney, Camperdown, Australia.

[8]Department of Infectious Diseases, Imperial College London, Medical School Building, St. Mary's Campus, London, United Kingdom.

Abstract

Kaposi sarcoma is a tumor caused by Kaposi sarcoma herpesvirus (KSHV) infection and is thought to originate from lymphatic endothelial cells (LEC). While KSHV establishes latency in virtually all susceptible cell types, LECs support spontaneous expression of oncogenic lytic genes, high viral genome copies, and release of infectious virus. It remains unknown the contribution of spontaneous virus production to the expansion of KSHV-infected tumor cells and the cellular factors that render the lymphatic environment unique to KSHV life cycle. We show here that

Corresponding Author: Päivi M. Ojala, Imperial College London, St. Mary's Campus, Norfolk Place, London W2 1PG, United Kingdom. Phone: 358-29-4159445; p.ojala@imperial.ac.uk.

K. Tuohinto and V. Nurminen contributed equally to this article.

Authors' Contributions

S. Gramolelli: Conceptualization, resources, data curation, formal analysis, supervision, funding acquisition, validation, investigation, methodology, writing-original draft, writing-review and editing. **E. Elbasani:** Conceptualization, resources, formal analysis, supervision, funding acquisition, validation, investigation, methodology, writing-review and editing. **K. Tuohinto:** Formal analysis, investigation, methodology. **V. Nurminen:** formal analysis, investigation, methodology. **T. Günther:** Data curation, formal analysis, methodology, writing-original draft. **R.E. Kallinen:** Formal analysis, investigation. **S.P. Kaijalainen:** Resources. **R. Diaz:** Validation, investigation. **A. Grundhoff:** Data curation, formal analysis. **C. Haglund:** Resources. **J.M. Ziegelbauer:** Formal analysis, writing-review and editing. **T. Pellinen:** Data curation, formal analysis, methodology, writing-review and editing. **M. Bower:** Resources, writing-review and editing. **M. Francois:** Conceptualization, resources, writing-review and editing. **P.M. Ojala:** Conceptualization, resources, supervision, funding acquisition, validation, writing-original draft, project administration, writing-review and editing.

Supplementary data for this article are available at Cancer Research Online (http://cancerres.aacrjournals.org/).

expansion of the infected cell population, observed in LECs, but not in blood endothelial cells, is dependent on the spontaneous virus production from infected LECs. The drivers of lymphatic endothelium development, SOX18 and PROX1, regulated different steps of the KSHV life cycle. SOX18 enhanced the number of intracellular viral genome copies and bound to the viral origins of replication. Genetic depletion or chemical inhibition of SOX18 caused a decrease of KSHV genome copy numbers. PROX1 interacted with ORF50, the viral initiator of lytic replication, and bound to the KSHV genome in the promoter region of ORF50, increasing its transactivation activity and KSHV spontaneous lytic gene expression and infectious virus release. In Kaposi sarcoma tumors, SOX18 and PROX1 expression correlated with latent and lytic KSHV protein expression. These results demonstrate the importance of two key transcriptional drivers of LEC fate in the regulation of the tumorigenic KSHV life cycle. Moreover, they introduce molecular targeting of SOX18 as a potential novel therapeutic avenue in Kaposi sarcoma.

Introduction

Oncogenic pathogens are responsible for 15% of all cancer cases (1). Seven viruses, one bacterium, and three parasites are recognized as well-established carcinogens by the International Agency for Research on Cancer (https://gco.iarc.fr/). Understanding the players involved in the oncogenic pathogen–host interactions is crucial to discover new therapies for these cancers.

Kaposi sarcoma is an angiogenic tumor caused by Kaposi sarcoma herpesvirus (KSHV). Kaposi sarcoma is the most common cancer in people living with HIV and a frequent malignancy in Sub-Saharan Africa, both in adults and children (2). Kaposi sarcoma presents with vascularized, multifocal skin lesions that progress from patch to plaque and ultimately to nodular tumors (3, 4). The histopathologic hallmark of Kaposi sarcoma is the presence and proliferation of KSHV-positive spindle cells (SC), the tumor cells of Kaposi sarcoma (3, 4). The cell of origin of SCs has long been debated (4). Recent studies point to a lymphatic endothelial origin (LEC), although mesenchymal and blood endothelial cells (BEC) can contribute to the SC population (2, 5). *In vitro*, latency has been considered the default replication program in KSHV-infected cells with undetectable expression of lytic genes. However, KSHV infection of lymphatic, but not blood, ECs leads to a unique infection program with spontaneous lytic gene expression and release of infectious virus (6–9). These features are crucial for Kaposi sarcoma tumorigenesis; on one hand, KSHV lytic genes encode oncogenic proteins whose expression in the tumor microenvironment accounts for Kaposi sarcoma pathogenic hallmarks, that is, abnormal inflammation, angiogenesis, and proliferation of SCs (4); on the other hand, it has been hypothesized that by releasing infectious virus that can infect the surrounding cells, the lytic reactivation is needed to replenish and expand the population of infected Kaposi sarcoma-SCs (10). This is supported by clinical evidence correlating the progression to advanced stage, nodular, Kaposi sarcoma with high blood levels of KSHV DNA (11, 12).

Here, we found that the infectious virus spontaneously released by KSHV-infected LEC (KLEC) can expand the population of infected cells in culture, providing further support for the importance of LECs in Kaposi sarcoma. Furthermore, we investigated which cellular

factors render the LEC environment so unique to KSHV expression program. Because the lymphatic, but not blood, endothelial environment supports the spontaneous lytic replication of KSHV, we hypothesized that the cellular factors that render LECs different from BECs in KSHV infection would be specific for or expressed at higher levels in LECs than BECs. We therefore addressed whether the transcription factors (TF), instrumental for LEC identity, would regulate also the features of KSHV infection program in LECs. During embryonic development, LEC precursors originate from COUPTF2/SOX18 double-positive venous BECs that separate from the cardinal vein to establish a primary lymphatic vascular plexus. COUPTF2 and SOX18 orchestrate LEC differentiation by driving *PROX1* expression (13, 14). Therefore, we investigated the role of PROX1, SOX18, and COUPTF2 in spontaneous lytic reactivation in KLECs.

We identified SOX18 and PROX1 as positive regulators of the KSHV infection program. SOX18 binds to the viral origins of replication and increases intracellular viral genome copies. Chemical inhibition or depletion of SOX18 reduced the number of viral genomes and infectious virus release. Conversely, PROX1 enhances the expression of KSHV lytic genes and virus release. We found that both these TFs are expressed in a series of 19 Kaposi sarcoma biopsies. SOX18 and PROX1 expression significantly correlated with the latent and lytic infection markers. These data demonstrate the importance of the LEC microenvironment for KSHV genome maintenance and spontaneous lytic replication and suggest that SOX18 and PROX1 are regulating the two key steps that directly contribute to the onset and progression of the disease.

Materials and Methods

Human subjects

Formalin fixed, paraffin-embedded (FFPE) Kaposi sarcoma sections were provided by Justin Weir (Charing Cross Hospital, and the London Clinic, London). The study (Kaposi's Sarcoma Herpes Virus Infection And Immunity, REC reference: 04/Q0401/80) was covered by Riverside Research Ethics Committee; all patients gave written informed consent.

FFPE Kaposi sarcoma–negative skin biopsies were obtained from the archives of the Department of Pathology, Helsinki University Hospital (Helsinki, Finland), according to the Finnish laws and regulations by permission of the director of the health care unit. The samples were deidentified and analyzed anonymously.

No experiments were performed on animals.

Cell culture

Primary human dermal lymphatic (C-12216) and blood (C-12211) ECs were purchased from Promocell and grown in Lonza EBM-2 (00190860) supplemented with EGM-2 MV Microvascular Endothelial SingleQuots (CC-4147), except for VEGF, which was not added. Cells were used until passage four. Each experiment was repeated using cells from two donors.

HEK293FT (Thermo Fisher Scientific, R70007; RRID:CVCL_6911), U2OS (ATCC:HTB-96; RRID:CVCL_0042), HeLa (ATCCCCL-2; RRID:CVCL_0030), and iSLK.219 (15) were grown in DMEM, supplemented with 10% FCS, 1% L-glutamate, 1% penicillin/streptomycin. iSLK.219 cells were also supplied with 10 μg/mL puromycin, 600 μg/mL hygromycin B, 400 μg/mL G418. Cells were used for approximately 15 passages. Cell lines were not authenticated by short tandem repeat profiling. Cells were regularly tested negative for *Mycoplasma* using Eurofins Mycoplasma Testing (last test was performed in February 2020).

IHC stainings, KSHV infection, lentiviruses production and transduction, DNA and siRNA transfection are described in refs. 8, 16, and in Supplementary Material and Methods.

Virus titration

One day prior to titration, 8,000 naïve U2OS/well were plated on viewPlate-96black (6005182, Perkin Elmer). Cells were spinoculated in the presence of 8 μg/mL of polybrene with serial dilution of precleared supernatant from infected cells. Cells were stained with antibodies against GFP (a kind gift from J. Mercer; UCL, London, United Kingdom) to detect the rKSHV.219-infected cells that express GFP from a cellular EF1α promoter or LANA (ab4103; Abcam) and Hoechst 33342.

Images from 9 fields/well were taken using Thermo Scientific Cell Insight High Content Screening System.

RNA sequencing

RNA from iSLK.219 cells and KLECs from three independent experiments, was extracted using NucleoSpin RNA extraction kit (Macherey Nagel). Ribosomal RNA was depleted using Ribo-zero rRNA Removal Kit (Illumina) and the RNA quality was monitored with Bioanalyzer RNA Kit (Agilent). Libraries were prepared using NEB Next-Ultra-Directional RNA library-Prep Kit for Illumina (NEB) and sequencing was done with NextSeq High-Output 1 × 75 bp. Data analysis is described in Supplementary Material and Methods

Raw data are deposited in the European nucleotide Archive (ID code: ena-STUDY-UNIVERSITY OF HELSINKI-13–02-2019–22:25: 30:309–452; accession number: PRJEB31253; http://www.ebi.ac.uk/ena/data/view/PRJEB31253).

Proximity ligation assay

Proximity ligation assay (PLA) was performed using Duolink PLA Technology (Sigma Aldrich) and antibodies against PROX1 (AF2727, R&D Systems) and ORF50 (a kind gift from C. Arias, University of California Santa Barbara, Santa Barbara, CA).

Luciferase reporter assay

Luciferase reporter assay was done as described in ref. 16. Further details in Supplementary Material and Methods.

Chromatin immunoprecipitation

For each immunoprecipitation (IP), one or three 10-cm dish for iSLK.219 and KLEC, respectively, and SimpleChIP Enzymatic Chromatin IP Kit (Cell Signaling Technology, 9003S) were used. Antibodies against PROX1 (11067–2-AP, ProteinTech Group), Myc (C2276, Cell Signaling Technology), SOX18 (sc-166025, Santa Cruz Biotechnology), normal mouse or rabbit IgG (sc-2025; sc-3888, Santa Cruz Biotechnology), and mouse monoclonal anti-HA.11(16B12, BD Pharmingen) were used.

The experiments were done at least two independent times. Isolated DNA was amplified with the primers listed in Supplementary Material and Methods.

Quantification of intracellular viral genome copies

DNA was isolated from cells using NucleoSpin Tissue Kit (74098, Macherey-Nagel) and analyzed by qPCR using primers for genomic actin (AGAAAATCTGGCACCACACC; AACGGCAGAAGAGAGAACCA) and K8.1 (AAAGCGTCCAGGCCACCACAGA; GGCAGAAAATGGCACACGGTTAC).

Inhibitor treatments

PAA, R-, S-, R-S-Propranolol (284270, P0689, P8688, P0884) were obtained from Sigma-Aldrich; SM4 was described in ref. 17.

Multiplexed IHC and image analysis

Multiplex mIHC was performed as described in ref. 18, with some modifications described in Supplementary Material and Methods.

For image analysis, red blood cell and tissue-derived autofluorescence was detected and removed by machine learning (Ilastik 1.3.3, Pixel classification). For this, RGB color images were generated from DAPI, FITC (K8.1), and CY3 (SOX18) channel images using CellProfiler GrayToColor module. All subsequent image analyses were performed using CellProfiler. Cells were segmented using Identify-PrimaryObjects for DAPI channel with Global threshold, minimum cross entropy, and 0.5 smoothing scale. All channels with a specific marker were thresholded using either manual cut-offs (K8.1) or Adaptive Otsu defined cut-offs (PROX1, SOX18, LANA). Cell classes were determined using MaskObjects modules.

Immunofluorescence, immunoblotting, qRT-PCR, siRNA, and DNA transfections and image analysis were described in ref. 16 and further details are given in Supplementary Material and Methods.

Statistical analysis

Data were analyzed with Prism GraphPad 8. Unless differently stated in the legend, the graphs show the single values of each biological replicate, the mean and the error bars indicate the SD across the biological replicates. Ordinary one-way ANOVA followed by Dunnett correction for multiple comparisons or two-tailed paired *t* test were performed to assess the statistical significance of the differences between samples.

After the mIHC image analysis, Pearson correlation coefficient between the markers was calculated and the *P* values to assess the significance of the correlation were calculated with two-tailed Student *t* test using SPSS software, false discovery rate was calculated using Bonferroni correction method.

Results

KLEC-derived virus spreads efficiently to naïve LECs but not to BECs

KSHV infection leads to different outcomes in LECs and BECs. The former displays a unique lytic expression program characterized by the expression of lytic proteins such as the late lytic protein K8.1 and the production of infectious virus, while the latter remains latent (6). We infected BECs or LECs for 14 days with rKSHV.219, a recombinant reporter virus strain expressing GFP from the EF1α cellular promoter and RFP from the viral lytic PAN promoter allowing detection of both latent (GFP^+) and lytic cells (RFP^+; ref. 19) or with a WT-KSHV strain (20). The expression of the late lytic protein K8.1 (Fig. 1A) and the production of high amount of infectious virus were detected from KSHV-LECs but not from KSHV-BECs (KLECs and KBECs; Fig. 1B). In addition, also the intracellular KSHV genome copy numbers (episomes) were significantly higher in KLECs than in KBECs (Fig. 1C).

Previous studies have shown that inefficient establishment of KSHV latency is due to the propensity of KSHV genomes to segregate viral genomes during cell division. For the progression of Kaposi sarcoma and the expansion of the tumor mass, infectious virus, the final product of the KSHV lytic cycle, is needed to replenish and increase the population of infected SCs. To test whether the infectious virus released by KLECs would support the expansion of the infected cell population, we mixed KLECs with either uninfected BECs or LECs (both possible Kaposi sarcoma-SCs precursors) at a ratio of 1:50. To assess the contribution of the infectious virus released from KLECs to the spread of infection, cells were also treated with phosphonoacetic acid (PAA), an inhibitor of viral but not cellular DNA polymerase, to block the production of infectious virus. We measured the percentage of infected cells 1, 3, and 7 days postinfection (d.p.i) by quantifying the percentage of infected (GFP-positive) cells (Fig. 1D). In the KLEC+BEC culture, the population of infected cells was approximately 2%–5% and no significant spreading of the infection was observed during the 7-day follow-up. In contrast, in the KLEC+LEC culture the population of infected cells increased to about 10% at three d.p.i. and 30% at seven d.p.i., while in the PAA-treated cultures the percentage of infected cells remained at the initial 2%–5%, suggesting that the increase in infected cells was due to the KLEC-derived virus reinfecting the naïve LECs.

To confirm this finding, we also measured the infectious virus spread in a KLEC culture infected at a low multiplicity of infection (MOI = 0.5) during a 14-day time-course in the presence or absence of PAA (Fig. 1E). While in the nontreated samples the infection spread to almost 100% of the cells, in the PAA-treated KLEC, the infection spread only moderately reaching about 20% by 14 d.p.i.

Overall, these results show that KLEC-derived virus can spread in a naïve LEC, but not in BEC culture, further suggesting that the efficient spontaneous lytic reactivation and virus production from KLECs could be the source of infection for the maintenance and expansion of the Kaposi sarcoma-SC population.

Endothelial-specific TFs and viral lytic genes are highly expressed in KLECs

Given the relevance of the spontaneous virus production from KLECs, we investigated the cellular factors responsible for the unique infection program in KLECs. Because neither lytic gene expression nor virus production were observed in KBECs, we hypothesized that cellular TFs specific for or expressed at higher levels in LECs than in BECs, could positively regulate the spontaneous lytic replication cycle in KLECs. We focused on PROX1, SOX18, and COUPTF2, the TFs that orchestrate the acquisition and maintenance of the LEC fate during embryogenesis and adulthood.

Oncogenic KSHV infection disturbs the LEC and BEC identity by skewing PROX1 expression profile in both KLECs and KBECs. In particular, *PROX1* transcription was shown to be upregulated in KBEC and downregulated in KLEC (21–25). However, neither SOX18 and COUPTF2 levels were previously analyzed nor PROX1 protein levels rigorously compared. Therefore, we analyzed the levels of PROX1, SOX18 and COUPTF2, together with infection (GFP), latent (LANA), and lytic (ORF50, ORF57, ORF45 and K8.1) markers either during a 14-day time course of infection (Fig. 2A and B; Supplementary Fig. S1A) or at 14 d.p.i. (Fig. 2C–E; Supplementary Fig. S1B and S1C). As reported previously (22, 23), *PROX1* transcripts, initially low in BECs, increased in KBECs up to 3-fold by 14 d.p.i. (Fig. 2A, top) and diminished to 4-fold in KLECs by 14 d.p.i. (Fig. 2A, bottom). KSHV infection increased *SOX18* transcripts in KBECs (3-fold by 10 d.p.i.) and KLECs (3-fold at 3 d.p.i.), while *COUPTF2* expression did not change (Fig. 2A). We observed modest expression of the lytic gene mRNAs in KBECs (Supplementary Fig. S1A), followed by their downregulation and the establishment of latency. In contrast to KBECs and in accordance with the unique infection program in KLECs, the lytic gene expression increased (Supplementary Fig. S1A), except at protein level at 10 d.p.i. where we consistently observed a downregulation of both viral proteins and the TFs studied, warranting further investigation (Fig. 2B, bottom).

Despite the transcriptional downregulation, comparable or even higher levels of PROX1 protein were detected by immunoblotting in KLECs compared with uninfected LECs upon infection with either rKSHV.219 (Fig. 2B, bottom and D) or WT-KSHV (Supplementary Fig. S1C) and further confirmed by immunofluorescence (Fig. 2E). SOX18 protein levels were increased in both KLECs and KBECs, while COUPTF2 levels increased in KLEC, but slightly decreased in KBEC (Fig. 2B, D, and E; Supplementary S1B and S1C).

Overall, the results show that SOX18, PROX1, and COUPTF2 were all highly expressed in KLECs compared with KBECs.

SOX18 and PROX1 regulate KSHV infection through different mechanisms

To investigate the role of SOX18, PROX1, and COUPTF2 in the unique KSHV infection program in KLECs, we assessed the effects of loss of function of these three TFs. Cells

treated with control siRNA or siRNAs targeting either of these three TFs for 72 hours were analyzed for: viral mRNAs, protein expression, and infectious virus release (Fig. 3A–C; Supplementary Fig. S2A–S2I). *PROX1* and *SOX18* gene knockdown significantly decreased the lytic transcript and protein levels, while *COUPTF2* depletion caused a modest increase in lytic gene expression. Of note, SOX18 depletion had a marked negative effect on *LANA* mRNA and protein levels while *PROX1* depletion halved *LANA* transcripts concentration, but only marginally reduced its protein levels (Fig. 3A and B; Supplementary Fig. S2A). The release of infectious KSHV (titer) was reduced by a half upon *PROX1* depletion and more severely after SOX18 silencing, while *COUPTF2* silencing did not have any effect on this, despite a decrease in lytic protein expression (Fig. 3B and C; Supplementary Fig. S2C, S2E, S2F, and S2H).

Because SOX18 depletion affected not only expression of the lytic genes, but also of the latent LANA, we investigated whether this was due to a diminished number of intracellular viral genomes. While *PROX1* silencing modestly decreased viral episomes by 10%, *SOX18* depletion by siRNAs decreased them by about 65% (Fig. 3D; Supplementary Fig. S2I), suggesting that SOX18 may contribute to the high episome copies in KLECs.

Next, we cosilenced *PROX1* and *SOX18* to test the combined effect of depleting these TFs on KSHV lytic replication cycle. As a positive control, we treated KLECs with PAA (Fig. 3E and F). As expected, PAA treatment slightly decreased transcription of the intermediate-early *ORF45* gene and more dramatically the late lytic gene *K8.1*, whereas *PROX1* and *SOX18* cosilencing reduced both early and late viral gene expression. Notably, the release of infectious virus was reduced more efficiently than their individual silencing and was comparable with the PAA treatment.

Interestingly, *PROX1* depletion in KLECs did not change SOX18 protein levels, whereas *SOX18* depletion decreased the *PROX1* mRNA and also its protein levels to some extent (Fig. 3B; Supplementary Fig. S2J). Because SOX18 positively regulates *PROX1* during LEC development, we explored the reciprocal effect of depletion of these TFs in uninfected LECs. Here, silencing of either *PROX1, SOX18*, or *COUPTF2* negatively affected the levels of all the other TFs. PROX1 expression decreased upon both SOX18 and COUPTF2 silencing recapitulating the molecular events that occurs in LEC progenitors during development. Similarly, lower SOX18 expression upon PROX1 and COUPTF2 depletion was observed in uninfected LECs (Supplementary Fig. S2K). This suggests that in KLECs KSHV infection has partially uncoupled the reciprocal regulation of PROX1, SOX18, and COUPTF2 expression.

These results show that the reciprocal regulation of PROX1 and SOX18 is partially uncoupled during KSHV infection. In turn, SOX18 and PROX1 both contribute to the unique infection program in KLECs via different mechanisms; SOX18 by controlling KSHV episome copies and PROX1 levels to some extent, and PROX1 by regulating viral lytic gene expression.

SOX18 inhibition efficiently decreases KSHV genome copies and infectious virus release

SOX18 homo- and heterodimerization can be inhibited by a small molecule, SM4 (17, 26) and by an FDA-approved beta blocker, propranolol (27). Propranolol is produced as a 1:1 racemic mixture of R(+) and S(−) enantiomers. The S(−) form exhibits beta-adrenergic blocking activity, while the less potent R(+) enantiomer is carried over during the drug synthesis. Similar to SM4, R(+) propranolol blocks SOX18 homo- and heterodimerization with RBPJ (27), as a result, SOX18 fails to regulate a subset of its endothelial-specific target genes (28).

Given the significant reduction in viral episomes and infectious virus release upon *SOX18* silencing in KLECs, we explored whether SM4 and R(+) propranolol would produce a similar outcome. KLECs were treated with SM4, the propranolol racemic mixture (R+S) or the pure enantiomers R(+) and S(−) (Fig. 4A–D) using the same range of concentrations that inhibits SOX18-mediated activation of EC-specific genes (28). We observed a dose-dependent decrease in KSHV intracellular episomes and released infectious virus in SM4 and R(+) propranolol-treated KLECs compared with the DMSO-treated control (Fig. 4A–D). The racemic mixture of propranolol and the S(−) enantiomer increased both KSHV episomes and virus titres. This finding agrees with a previous report (29), where propranolol treatment of immortalized KLECs induced to lytic replication cycle by phorbol esters increased lytic KSHV released virus, likely by interfering with the cell cycle rather than having a SOX18-specific inhibitory effect.

To further assess the specificity of the inhibitors, we tested these drugs on the SOX18-negative iSLK.219 cells transduced with a mCherry control (Myc-NLS-mCherry) or a Myc-tagged SOX18-expressing lentivirus. iSLK.219 is a cancer cell line stably infected with rKSHV.219 and harboring a doxycycline-inducible KSHV-*ORF50* that drives lytic reactivation (15). In the absence of doxycycline, these cells are latent. KSHV episomes were quantified in latently infected cells or cells reactivated with doxycycline for 48 hours and treated with the indicated inhibitors or DMSO (Fig. 4E). SOX18 expression significantly increased the numbers of KSHV episomes in both latent and lytic cells. SM4 and R(+) propranolol treatments reduced episome copies in iSLK.219 ectopically expressing SOX18, but not in the controls, supporting the specificity of the SOX18 inhibition.

These results provide a proof of principle that targeting SOX18 could represent a novel molecular strategy for Kaposi sarcoma treatment.

SOX18 binds to the KSHV genome in the proximity of the origins of replication

To complement our observations and further investigate the effect of SOX18 on the KSHV episome copy number, KBECs, which express low levels of SOX18, were transduced with lentiviruses expressing either SOX18 or the mCherry control. The increase in SOX18 expression was confirmed by immunoblotting and the KSHV genome copies quantified after 72 hours (Fig. 5A). In the SOX18-expressing KBECs, we detected almost three times more KSHV genomes than in the control. Moreover, a significant, dose-dependent increase of KSHV episomes over the mCherry-transduced control was observed when iSLK.219 cells were transduced with increasing amounts of SOX18-expressing lentiviruses for 48

hours (Fig. 5B). The expression level of SOX18 protein was compared with the levels in KLECs to ensure that SOX18 levels remained reasonably similar to the endogenous levels in KLEC. By 5-ethynyl-2′-deoxyuridine (EdU) assay, we confirmed that the increase in KSHV episomes was not due to increased proliferation of SOX18-expressing iSLK.219 (Supplementary Fig. S3A). In addition, KSHV gene, protein expression, and released virus were monitored for 72 hours in iSLK.219 after doxycycline-induced reactivation (Supplementary Fig. S3B–D). SOX18 ectopic expression moderately increased KSHV lytic transcripts and proteins without increasing the virus titers. These data suggest that SOX18 expression increases viral genome copies without increasing cell proliferation and only slightly contributes to lytic gene expression upon doxycycline induction.

Because SOX18 depletion decreased KSHV episome copies in KLECs, and conversely its ectopic expression increased the number of viral episomes in KBECs and iSLK.219 cells, we tested whether SOX18 would bind to the viral episomes in the proximity of the origins of replication. During latency, KSHV replicates mainly by a LANA-dependent mechanism from the terminal-repeat (TR) region of the KSHV genome and, to a minor extent, through a LANA-independent mechanism from the OriA region, adjacent to the origin of lytic replication (OriLyt; refs. 30, 31). To address whether SOX18 would directly bind to the KSHV origins of replication, we used reporter plasmids harboring either seven copies of the TR region (7XTR) or the OriA fused to OriLyt upstream of an SV40 promoter fused to a firefly luciferase reporter (Fig. 5C and D; Supplementary Fig. S3E and S3F). In the presence of LANA, SOX18 expression increased the activity of the 7XTR-luc reporter in a dose-dependent manner. ORF50 that binds to the OriLyt and is a potent activator of the OriA+OriLyt-luc reporter (32), was used as a positive control for this assay. Interestingly, SOX18 expression also increased the activity of the OriA+OriLyt-luc reporter, but in an ORF50-independent manner. Moreover, SOX18 did not change the activity of a reporter plasmid harboring the *ORF50* promoter (Supplementary Fig. S3G), supporting the SOX18 specificity in the activation observed with the 7XTR- and OriA+OriLyt-luc reporters.

Because the reporter assays suggested that SOX18 binds to the KSHV origins of replication, we assessed this by chromatin immunoprecipitation (ChIP)-qPCR both in KLECs, in the presence of endogenous SOX18 (Fig. 5E–G, middle) and in iSLK.219 ectopically expressing a Myc-tagged SOX18 (Fig. 5E–G, bottom). Binding of SOX18 to the KSHV genome was observed in regions adjacent to the TR and within and adjacent to the OriA region in both KLECs using an anti-SOX18 antibody and in Myc-tagged SOX18-transduced iSLK.219 cells using an anti-Myc antibody. SOX18 drives EC fate through the regulation of a subset of genes harboring in their promoter an IR5 consensus motif, composed of two inverted SOX18-binding motifs spaced by five nucleotides (28). Notably, one of these motifs was adjacent to the KSHV TR region bound by SOX18 (Fig. 5E, top).

Overall these results indicate that SOX18 increases viral episome copies when ectopically expressed in KSHV-infected cells with low or no SOX18 expression. We further demonstrate direct binding of SOX18 in the proximity of KSHV origins of replication both in KLECs and iSLK.219 cells.

PROX1 enhances viral gene expression, interacts with ORF50, and binds to its promoter region during KSHV lytic replication cycle

To obtain a comprehensive picture of the PROX1-mediated KSHV lytic gene regulation, we performed loss and gain of PROX1 function and measured the cell response by transcriptomic profiling. We performed RNA-seq of KLECs transfected for 72 hours with either control or PROX1-targeting siRNA and doxycycline-treated (24 hours) iSLK.219 cells expressing a Myc-tagged PROX1 from a lentivirus. Efficient PROX1 silencing (with siRNAs used in Fig. 3 and Supplementary Fig. S2A–S2C and S2J) in KLECs reduced the expression of all KSHV genes and circular RNAs, expressed during the lytic cycle (Fig. 6A, left; Supplementary Fig. S4A; refs. 33, 34). Analysis of differentially expressed genes (DE-Seq DEG analysis Supplementary Table S1) revealed several cellular pathways involved in oncogenesis (e.g., p53 signaling, viral carcinogenesis, and transcriptional misregulation in cancer) altered by PROX1 silencing in KLECs (Supplementary Fig. S4B), supporting the pivotal role of PROX1 for KSHV gene expression and in Kaposi sarcoma tumorigenesis. Conversely, PROX1 reintroduction into iSLK.219 cells induced with doxycycline led to an overall increase in viral gene expression (Fig. 6A, right). The analysis of DEG (Supplementary Table S2) in iSLK.219 cells ± PROX1 did not identify differentially regulated pathways.

We further characterized iSLK.219 cells transduced with lentiviruses encoding a Myc-tagged PROX1, either WT or a mutant (MUT) harboring two point mutations at the DNA binding site (N624A and N626A) and lacking transcriptional activity (35), as well as a control vector. One day after doxycycline-induced lytic reactivation PROX1 WT, but not MUT, expression increased the transcription of lytic KSHV genes and immunoblot analysis revealed higher lytic protein levels in the presence of PROX1 WT (Supplementary Fig. S4C and S4D). High-content image analysis of iSLK.219 cells 24 hours after doxycycline-induced reactivation, revealed that PROX1 WT, but not MUT, increased the percentage of cells positive for early (RFP, ORF57) and late (K8.1) lytic markers (Supplementary Fig. S4E). iSLK.219 cells expressing PROX1 WT produced significantly higher infectious virus titers when compared with MUT or controls (Supplementary Fig. S4F). To assess whether PROX1 could induce spontaneous lytic reactivation in latent iSLK.219, they were transduced with PROX1 (either WT or MUT) lentiviruses or controls in the absence of doxycycline. This led to a 2- to 10-fold increase in viral lytic gene mRNAs, but did not increase lytic proteins to a detectable level (Supplementary Fig. S4G and S4H). The effect of PROX1 WT or MUT ectopic expression was assessed also in KLECs and KBECs where, in agreement with the iSLK.219 data, we observed an increase in viral lytic gene expression upon PROX1 WT but not MUT reintroduction (Fig. 6B).

These results suggest that, upon lytic reactivation, transcriptionally active PROX1 increases KSHV lytic gene expression.

Because PROX1 introduction into iSLK.219 cells led to a global increase in the expression of KSHV lytic genes already 24 hours after ORF50 induction by doxycycline, we hypothesized that an early viral lytic factor was needed for PROX1 to significantly enhance the KSHV lytic replication cycle. Because KSHV ORF50 can trigger the complete lytic cascade, we investigated whether PROX1 would act synergistically with ORF50 to increase

the lytic gene expression. We first performed a luciferase reporter assay using the *ORF50* promoter fused upstream of a luciferase gene (*ORF50*-luc) and measured its activity upon ectopic expression of PROX1, WT, or MUT, or ORF50 expression plasmid alone and in combination (Fig. 6C; Supplementary Fig. S4I). PROX1 alone did not increase the *ORF50* promoter activity above the basal levels, in agreement with its inability to induce a strong reactivation in latent iSLK.219 cells. However, PROX1 WT, but not MUT, significantly enhanced the *ORF50*-induced transcription from its own promoter. We further explored the PROX1-ORF50 potential physical interaction in KLECs and found that ORF50 coimmunoprecipitated with anti-PROX1 antibody in KLECs (Fig. 6D). We also observed that a Myc-tagged PROX1 WT, and to a minor extent a Myc-tagged PROX1 MUT, coimmunoprecipitated ORF50 in iSLK.219 reactivated for 24 hours by doxycycline treatment (Supplementary Fig. S4J). Similarly, streptactin-tagged ORF50 coprecipitated both PROX1 WT and MUT in HEK293FT cells (Supplementary Fig. S4K). Furthermore, in LECs infected with WT-KSHV, ORF50, and PROX1 colocalized in the viral replication and transcription compartments (Pearson correlation coefficient, PCC = 0.65, Fig. 6E; refs. 36, 37). This interaction was further confirmed in KLECs by PLA using ORF50 and PROX1-specific antibodies and analysis of more than 200 cells showing that the number of PLA puncta per nucleus were significantly higher than in the IgG-stained control (Fig. 6F). To test whether PROX1 binds to the *ORF50* promoter in KSHV-infected cells, ChIP was performed in iSLK.219 cells (latent or doxycycline-induced for 24 hours) to precipitate the Myc-tagged PROX1-bound chromatin with two different antibodies (anti-PROX1 and anti-Myc) followed by qRT-PCR to amplify the *ORF50* promoter region up to 850 nt upstream of the *ORF50* TSS. PROX1 bound to the proximal regions of the *ORF50* promoter during the lytic cycle (Fig. 6G, middle), but not during latency (Supplementary Fig. S4L). PROX1 binding to the *ORF50* promoter was also confirmed in KLECs (Fig. 6G, bottom).

These data indicate that PROX1 enhances KSHV lytic gene expression, binds to the initiator of the lytic replication cycle, ORF50, and during the lytic cycle it binds to the *ORF50* promoter. PROX1 also enhances the autoactivation of *ORF50* promoter in an ORF50-dependent manner.

PROX1, SOX18, COUPTF2, and K8.1 are expressed in Kaposi sarcoma tumors

Here we have demonstrated that PROX1 and SOX18, but not COUPTF2 contribute to the unique infection program in KLECs. To investigate whether these three TFs were expressed in Kaposi sarcoma tumors consecutive sections of biopsies from four patients with AIDS-Kaposi sarcoma were stained with anti-PROX1, -SOX18, and -COUPTF2 antibodies and their expression was compared with skin from Kaposi sarcoma–negative donors. While PROX1 expression in Kaposi sarcoma tumors has been shown previously (16, 22, 23, 38), SOX18 and COUPTF2 expression has not been reported. Adjacent sections were also stained for LANA and K8.1, markers of KSHV latent and lytic infection, respectively. SOX18, PROX1, and COUPTF2 were prominently expressed in all Kaposi sarcoma biopsies analyzed (Fig. 7A; Supplementary Fig. S5A) while in the Kaposi sarcoma-negative skin samples their expression was restricted to the endothelium lining the vessels, as expected (Supplementary Fig. S5B). No signals were detected on normal skin with anti-K8.1 antibody

(Supplementary Fig. S5C), or using isotype control antibodies on Kaposi sarcoma sections, confirming the specificity of the stainings (Supplementary Fig. S5D).

To demonstrate that PROX1 and SOX18 were expressed in the same cells with LANA and K8.1 in Kaposi sarcoma biopsies, we performed multiplex IHC of a cohort of 19 skin Kaposi sarcoma cases (including four HIV-negative cases) followed by quantitative image analysis of 8,345 tumor cells. Within the tumors we observed lytically infected cells, positive for both LANA and K8.1 (highlighted by orange arrowheads in Fig. 7B; Supplementary Fig. S5E), cells latently infected that were positive for LANA but not for K8.1 (indicated by white arrowheads in Fig. 7B; Supplementary Fig. S5E), as well as uninfected cells, negative for both LANA and K8.1 (marked with cyan arrowheads in Fig. 7B; Supplementary Fig. S5E). Quantification of signal intensity revealed that SOX18 expression significantly correlated with LANA expression (Fig. 7C) and PROX1 staining positively correlated with both K8.1 and LANA expression (Fig. 7D; Supplementary Fig. S5F), indicating that PROX1 and SOX18 are expressed in KSHV-infected Kaposi sarcoma tumor cells. In addition, K8.1 expression was significantly higher in the LANA-positive (i.e., infected) cells (Fig. 7D) suggestive on an ongoing lytic replication in Kaposi sarcoma tumor cells.

Overall, our data shows that SOX18 and PROX1 are expressed in Kaposi sarcoma-SCs positive for LANA and K8.1 proteins, thus supporting the relevance of these TFs in the oncogenic KSHV life cycle also in Kaposi sarcoma.

Discussion

KSHV infection of BECs or LECs results in different viral expression programs in the infected cells. While the virus is latent in BECs, it displays a unique, spontaneously lytic replication program in LECs (6). We found that SOX18 and PROX1, TFs essential for LECs identity maintenance, are expressed in Kaposi sarcoma tumors and regulate the KSHV life cycle through two different mechanisms (Fig. 7E). COUPTF2, also expressed in Kaposi sarcoma, displayed a relatively low involvement of KSHV replication in KLECs. Differently from the uninfected LECs, SOX18, PROX1, and COUPTF2 expressions are not interdependent in KLECs. KSHV infection uncouples their reciprocal regulation and maintains high levels of these TFs and, in turn, SOX18 and PROX1 sustain viral infection. This suggests that KSHV modulates the cellular microenvironment for its own persistence. Although KSHV infection also increases SOX18 and PROX1 levels in BECs this, however, is not sufficient to sustain the unique spontaneously lytic replication program seen in KLECs. In fact, SOX18 and PROX1 were found to increase the episome copies and the lytic replication, respectively, only when ectopically expressed in KBECs. Overall this may indicate that KSHV infection is skewing LECs and BECs toward a LEC-embryonic phenotype, when during the early steps of lymphangiogenesis, these three TFs are initiating the LEC differentiation program.

Furthermore, we show that the late lytic protein K8.1 is expressed in KSHV-positive tumor cells in a series of 19 Kaposi sarcoma cases, suggesting that lytic protein expression is common in Kaposi sarcoma. The correlation of latent and lytic protein expression with

SOX18 and PROX1 in Kaposi sarcoma suggests that these factors could regulate KSHV life cycle also *in vivo.*

Viral persistence and lytic replication are necessary to support Kaposi sarcoma tumorigenesis for two reasons (3, 4, 39, 40). First, KSHV encodes an arsenal of lytic oncogenes such as viral-encoded inflammatory cytokines, membrane proteins deregulating proliferation, angiogenesis, inflammatory signaling and secretome of infected ECs (2, 4). Second, KSHV genome maintenance is inefficient and viral genomes are lost during cell division (10, 41). Sporadic lytic reactivation and release of infectious virus may be required *in vivo* to replenish and expand the population of KSHV-infected Kaposi sarcoma-SCs. Here we show that the spontaneous virus production from KLECs is needed to spread the infection to cocultured, uninfected LECs (Fig. 7E, left). In addition, SOX18 and PROX1 were identified here as positive regulators of viral genome copies and productive lytic replication, respectively (Fig. 7E, right).

SOX18 is recognized among the genes differentially regulated in Kaposi sarcoma tumors compared with normal skin (24), but its role in the KSHV biology has been little explored. So far, SOX18 has only been linked to the transcriptional regulation of ECs and to the progression of solid cancers (42, 43), and this is the first time it has been ascribed a role in the life cycle of an oncogenic virus. SOX18 forms a dimer (17, 28), that binds viral and cellular DNA. This could contribute to a stronger tethering of the viral episomes to the host genome, thus improving their retention. Supporting this is the finding that inhibition of SOX18 homo- and heterodimerization reduced the number of intracellular KSHV genomes. It is also possible that SOX18 acts as a pioneering TF that renders the viral chromatin more prone for genome replication. While the less characterized SM4 will need further testing, the enantiopure R propranolol has already been proven safe (44) and could in principle be repurposed to treat Kaposi sarcoma.

This study underscores the importance of SOX18 and PROX1 in Kaposi sarcoma tumorigenesis as they contribute to replenish and maintain the population of KSHV-infected SCs. Moreover, through positive regulation of the lytic gene expression program, these TFs support the expression of angiogenic and inflammatory viral genes that are necessary to sustain tumorigenesis in the infected microenvironment.

Supplementary Material

Refer to Web version on PubMed Central for supplementary material.

Acknowledgments

We are grateful to Paul Farrell for critical comments on the manuscript and to Takanobu Takawa for the technical support in the detection of Kcirc RNAs. We acknowledge Kari Alitalo (University of Helsinki, Helsinki, Finland) for providing valuable reagents, tools, and advice. We thank the Biomedicum Imaging Unit (BIU) and Genome Biology Unit (GBU) at the University of Helsinki for support in imaging and the Digital and Molecular Pathology Unit supported by Helsinki University and Biocenter Finland for digital microscopy services as well as the Functional Genomic Unit (FuGU, University of Helsinki, Helsinki, Finland) for technical support during the RNA-seq. Justin Weir (Imperial College Healthcare NHS Trust) is acknowledged for kindly providing the Kaposi sarcoma biopsies. We are also extremely grateful to Nadezhda Zinovkina, Elina Hurskainen, Annabrita Schoonenberg, and Pia Saarinen (University of Helsinki) for the valuable technical help. Bala Chandran (University of South Florida) and Carolina Arias (University of California Santa Barbara, Santa Barbara, CA) are thanked

for antibodies to LANA and ORF50, respectively. The study was supported by the Academy of Finland Centre of Excellence Program for years 2014–2019, Translational Cancer Biology, grant no. 307366 (to P.M. Ojala) and the Academy of Finland postdoctoral researcher posts (grant no. 309544 to S. Gramolelli; 324487 to E. Elbasani), Finnish Cancer Foundations (to P.M. Ojala), and Sigrid Juselius Foundation (to P.M. Ojala). K. Tuohinto was supported by the Doctoral Programme in Biomedicine (DPBM), University of Helsinki. M. Francois is a NHMRC CDF (1111169) and his research is funded from NHMRC 1164000.

Disclosure of Potential Conflicts of Interest

M. Francois reports personal fees from Gertrude Biomedical Pty Ltd (scientific advisor for GBM-consulting fees) outside the submitted work. In addition, M. Francois has a patent for SOX18 small-molecule inhibitors licensed to Gertrude Biomedical (early days for the start up; no royalties have been provided). P.M. Ojala reports grants from Academy of Finland (Centre of Excellence Program and two postdoctoral posts), Finnish Cancer Foundation, and Sigrid Juselius Foundation during the conduct of the study. No potential conflicts of interest were disclosed by the other authors.

References

1. Plummer M, de Martel C, Vignat J, Ferlay J, Bray F, Franceschi S. Global burden of cancers attributable to infections in 2012: a synthetic analysis. Lancet Glob Health 2016;4:e609–16. [PubMed: 27470177]
2. Gramolelli S, Schulz TF. The role of Kaposi sarcoma-associated herpesvirus in the pathogenesis of Kaposi sarcoma. J Pathol 2015;235:368–80. [PubMed: 25212381]
3. Ojala PM, Schulz TF. Manipulation of endothelial cells by KSHV: implications for angiogenesis and aberrant vascular differentiation. Semin Cancer Biol 2014;26:69–77. [PubMed: 24486643]
4. Gramolelli S, Ojala PM. Kaposi's sarcoma herpesvirus-induced endothelial cell reprogramming supports viral persistence and contributes to Kaposi's sarcoma tumorigenesis. Curr Opin Virol 2017;26:156–62. [PubMed: 29031103]
5. Li Y, Zhong C, Liu D, Yu W, Chen W, Wang Y, et al. Evidence for Kaposi Sarcoma originating from mesenchymal stem cell through KSHV-induced mesenchymal-to-endothelial transition. Cancer Res 2018;78:230–45. [PubMed: 29066510]
6. Chang HH, Ganem D. A unique herpesviral transcriptional program in KSHV-infected lymphatic endothelial cells leads to mTORC1 activation and rapamycin sensitivity. Cell Host Microbe 2013;13:429–40. [PubMed: 23601105]
7. Yogev O, Boshoff C. Redefining KSHV latency. Cell Host Microbe 2013;13:373–4. [PubMed: 23601098]
8. Cheng F, Pekkonen P, Laurinavicius S, Sugiyama N, Henderson S, Gunther T, et al. KSHV-initiated notch activation leads to membrane-type-1 matrix metalloproteinase-dependent lymphatic endothelial-to-mesenchymal transition. Cell Host Microbe 2011;10:577–90. [PubMed: 22177562]
9. Golas G, Alonso JD, Toth Z. Characterization of de novo lytic infection of dermal lymphatic microvascular endothelial cells by Kaposi's sarcoma-associated herpesvirus. Virology 2019;536:27–31. [PubMed: 31394409]
10. Grundhoff A, Ganem D. Inefficient establishment of KSHV latency suggests an additional role for continued lytic replication in Kaposi sarcoma pathogenesis. J Clin Invest 2004;113:124–36. [PubMed: 14702116]
11. Campbell TB, Borok M, Gwanzura L, MaWhinney S, White IE, Ndemera B, et al. Relationship of human herpesvirus 8 peripheral blood virus load and Kaposi's sarcoma clinical stage. AIDS 2000;14:2109–16. [PubMed: 11061651]
12. Quinlivan EB, Zhang C, Stewart PW, Komoltri C, Davis MG, Wehbie RS. Elevated virus loads of Kaposi's sarcoma-associated human herpesvirus 8 predict Kaposi's sarcoma disease progression, but elevated levels of human immunodeficiency virus type 1 do not. J Infect Dis 2002;185:1736–44. [PubMed: 12085319]
13. Francois M, Caprini A, Hosking B, Orsenigo F, Wilhelm D, Browne C, et al. Sox18 induces development of the lymphatic vasculature in mice. Nature 2008; 456:643–7. [PubMed: 18931657]
14. Srinivasan RS, Geng X, Yang Y, Wang Y, Mukatira S, Studer M, et al. The nuclear hormone receptor Coup-TFII is required for the initiation and early maintenance of Prox1 expression in lymphatic endothelial cells. Genes Dev 2010;24: 696–707. [PubMed: 20360386]

15. Myoung J, Ganem D. Generation of a doxycycline-inducible KSHV producer cell line of endothelial origin: maintenance of tight latency with efficient reactivation upon induction. J Virol Methods 2011;174:12–21. [PubMed: 21419799]
16. Gramolelli S, Cheng J, Martinez-Corral I, Vaha-Koskela M, Elbasani E, Kaivanto E, et al. PROX1 is a transcriptional regulator of MMP14. Sci Rep 2018;8:9531. [PubMed: 29934628]
17. Fontaine F, Overman J, Moustaqil M, Mamidyala S, Salim A, Narasimhan K, et al. Small-molecule inhibitors of the SOX18 transcription factor. Cell Chem Biol 2017;24:346–59. [PubMed: 28163017]
18. Blom S, Paavolainen L, Bychkov D, Turkki R, Maki-Teeri P, Hemmes A, et al. Systems pathology by multiplexed immunohistochemistry and whole-slide digital image analysis. Sci Rep 2017;7:15580. [PubMed: 29138507]
19. Vieira J, O'Hearn PM. Use of the red fluorescent protein as a marker of Kaposi's sarcoma-associated herpesvirus lytic gene expression. Virology 2004;325:225–40. [PubMed: 15246263]
20. Nakamura H, Lu M, Gwack Y, Souvlis J, Zeichner SL, Jung JU. Global changes in Kaposi's sarcoma-associated virus gene expression patterns following expression of a tetracycline-inducible Rta transactivator. J Virol 2003;77:4205–20. [PubMed: 12634378]
21. Cancian L, Hansen A, Boshoff C. Cellular origin of Kaposi's sarcoma and Kaposi's sarcoma-associated herpesvirus-induced cell reprogramming. Trends Cell Biol 2013;23:421–32. [PubMed: 23685018]
22. Hong YK, Foreman K, Shin JW, Hirakawa S, Curry CL, Sage DR, et al. Lymphatic reprogramming of blood vascular endothelium by Kaposi sarcoma-associated herpesvirus. Nat Genet 2004;36:683–5. [PubMed: 15220917]
23. Yoo J, Lee HN, Choi I, Choi D, Chung HK, Kim KE, et al. Opposing regulation of PROX1 by interleukin-3 receptor and NOTCH directs differential host cell fate reprogramming by Kaposi sarcoma herpes virus. PLoS Pathog 2012;8:e1002770. [PubMed: 22719258]
24. Wang HW, Trotter MW, Lagos D, Bourboulia D, Henderson S, Makinen T, et al. Kaposi sarcoma herpesvirus-induced cellular reprogramming contributes to the lymphatic endothelial gene expression in Kaposi sarcoma. Nat Genet 2004;36:687–93. [PubMed: 15220918]
25. Carroll PA, Brazeau E, Lagunoff M. Kaposi's sarcoma-associated herpesvirus infection of blood endothelial cells induces lymphatic differentiation. Virology 2004;328:7–18. [PubMed: 15380353]
26. Overman J, Fontaine F, Moustaqil M, Mittal D, Sierecki E, Sacilotto N, et al. Pharmacological targeting of the transcription factor SOX18 delays breast cancer in mice. Elife 2017;6:e21221. [PubMed: 28137359]
27. Overman J, Fontaine F, Wylie-Sears J, Moustaqil M, Huang L, Meurer M, et al. R-propranolol is a small molecule inhibitor of the SOX18 transcription factor in a rare vascular syndrome and hemangioma. Elife 2019;8:e43026. [PubMed: 31358114]
28. Moustaqil M, Fontaine F, Overman J, McCann A, Bailey TL, Rudolffi Soto P, et al. Homodimerization regulates an endothelial specific signature of the SOX18 transcription factor. Nucleic Acids Res 2018;46:11381–95. [PubMed: 30335167]
29. McAllister SC, Hanson RS, Manion RD. Propranolol decreases proliferation of endothelial cells transformed by Kaposi's sarcoma-associated herpesvirus and induces lytic viral gene expression. J Virol 2015;89:11144–9. [PubMed: 26269192]
30. Verma SC, Lan K, Choudhuri T, Cotter MA, Robertson ES. An autonomous replicating element within the KSHV genome. Cell Host Microbe 2007;2:106–18. [PubMed: 18005725]
31. Verma SC, Lu J, Cai Q, Kosiyatrakul S, McDowell ME, Schildkraut CL, et al. Single molecule analysis of replicated DNA reveals the usage of multiple KSHV genome regions for latent replication. PLoS Pathog 2011;7:e1002365. [PubMed: 22072974]
32. Chen J, Ye F, Xie J, Kuhne K, Gao SJ. Genome-wide identification of binding sites for Kaposi's sarcoma-associated herpesvirus lytic switch protein, RTA. Virology 2009;386:290–302. [PubMed: 19233445]
33. Tagawa T, Gao S, Koparde VN, Gonzalez M, Spouge JL, Serquina AP, et al. Discovery of Kaposi's sarcoma herpesvirus-encoded circular RNAs and a human antiviral circular RNA. Proc Natl Acad Sci U S A 2018;115:12805–10. [PubMed: 30455306]

34. Toptan T, Abere B, Nalesnik MA, Swerdlow SH, Ranganathan S, Lee N, et al. Circular DNA tumor viruses make circular RNAs. Proc Natl Acad Sci U S A 2018;115:E8737–E45. [PubMed: 30150410]

35. Petrova TV, Makinen T, Makela TP, Saarela J, Virtanen I, Ferrell RE, et al. Lymphatic endothelial reprogramming of vascular endothelial cells by the Prox1 homeobox transcription factor. EMBO J 2002;21:4593–9. [PubMed: 12198161]

36. Baquero-Perez B, Whitehouse A.Hsp70 isoforms are essential for the formation of Kaposi's sarcoma-associated herpesvirus replication and transcription compartments. PLoS Pathog 2015;11:e1005274. [PubMed: 26587836]

37. Schmid M, Speiseder T, Dobner T, Gonzalez RA. DNA virus replication compartments. J Virol 2014;88:1404–20. [PubMed: 24257611]

38. Miettinen M, Wang ZF. Prox1 transcription factor as a marker for vascular tumors-evaluation of 314 vascular endothelial and 1086 nonvascular tumors. Am J Surg Pathol 2012;36:351–9. [PubMed: 22067331]

39. Barillari G, Sgadari C, Palladino C, Gendelman R, Caputo A, Morris CB, et al. Inflammatory cytokines synergize with the HIV-1 Tat protein to promote angiogenesis and Kaposi's sarcoma via induction of basic fibroblast growth factor and the alpha v beta 3 integrin. J Immunol 1999;163:1929–35. [PubMed: 10438928]

40. Biberfeld P, Ensoli B, Sturzl M, Schulz TF. Kaposi sarcoma-associated herpesvirus/human herpesvirus 8, cytokines, growth factors and HIV in pathogenesis of Kaposi's sarcoma. Curr Opin Infect Dis 1998;11:97–105. [PubMed: 17033372]

41. Chiu YF, Sugden AU, Fox K, Hayes M, Sugden B. Kaposi's sarcoma-associated herpesvirus stably clusters its genomes across generations to maintain itself extrachromosomally. J Cell Biol 2017;216:2745–58. [PubMed: 28696226]

42. Francois M, Harvey NL, Hogan BM. The transcriptional control of lymphatic vascular development. Physiology 2011;26:146–55. [PubMed: 21670161]

43. Olbromski M, Podhorska-Okolow M, Dziegiel P. Role of the SOX18 protein in neoplastic processes. Oncol Lett 2018;16:1383–9. [PubMed: 30008814]

44. Stensrud P, Sjaastad O. Short-term clinical trial of phopranolol in racemic form (Inderal), D-propranolol and placebo in migraine. Acta Neurol Scand 1976;53:229–32. [PubMed: 773081]

Significance:

SOX18 and PROX1, central regulators of lymphatic development, are key factors for KSHV genome maintenance and lytic cycle in lymphatic endothelial cells, supporting Kaposi sarcoma tumorigenesis and representing attractive therapeutic targets.

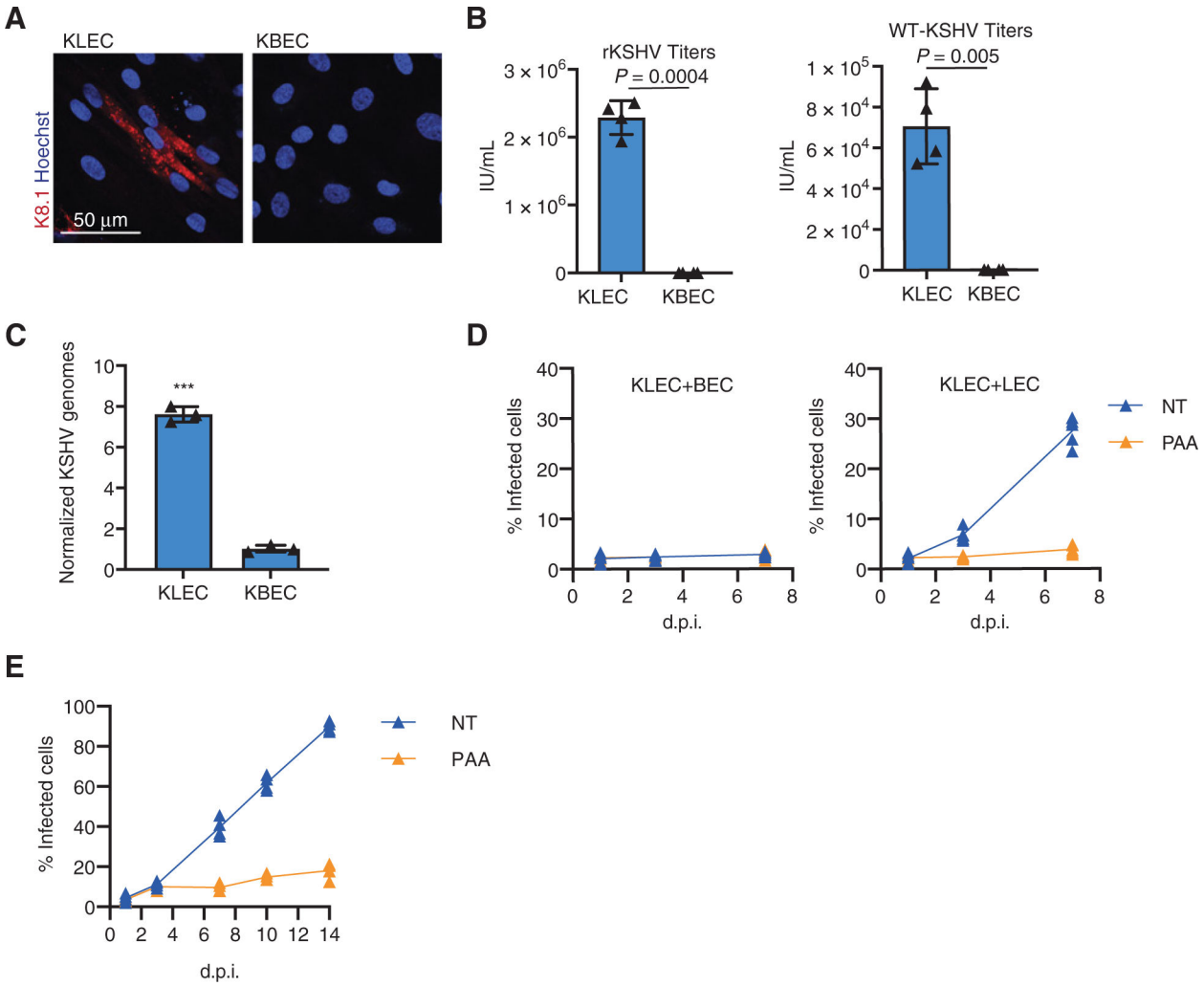

Figure 1.

Spontaneous virus production from KLECs supports virus spread in LECs. **A,** Immunofluorescence staining in the indicated cell types at 14 d.p.i. for K8.1 (red). Nuclei are counterstained with Hoechst 33342. Representative images from two independent experiments are shown. **B,** Titration of infectious virus released from KBECs and KLECs at 14 d.p.i. Infected U2OS target cells were quantified by their GFP expression. Single values from $n = 4$ biological replicates are shown. Bars, mean ± SD. P value was calculated using two-tailed paired t test. **C,** Quantification of intracellular viral genome copies from KBECs and KLECs at 14 d.p.i. Single values from $n = 3$ biological replicates are shown. Bars, mean ± SD. **D,** KLECs were mixed with noninfected BECs (left) or LECs (right) at a ratio of 1:50; three days later, PAA was added. At the indicated timepoints the percentage of infected (GFP^+) cells was quantified. Each dot represents one biological replicate. **E,** Left, LECs were infected at low multiplicity of infection (MOI) 0.5, and at three d.p.i., PAA was added. At the indicated timepoints, the percentages of GFP^+ cells were quantified. Each dot represents one biological replicate.

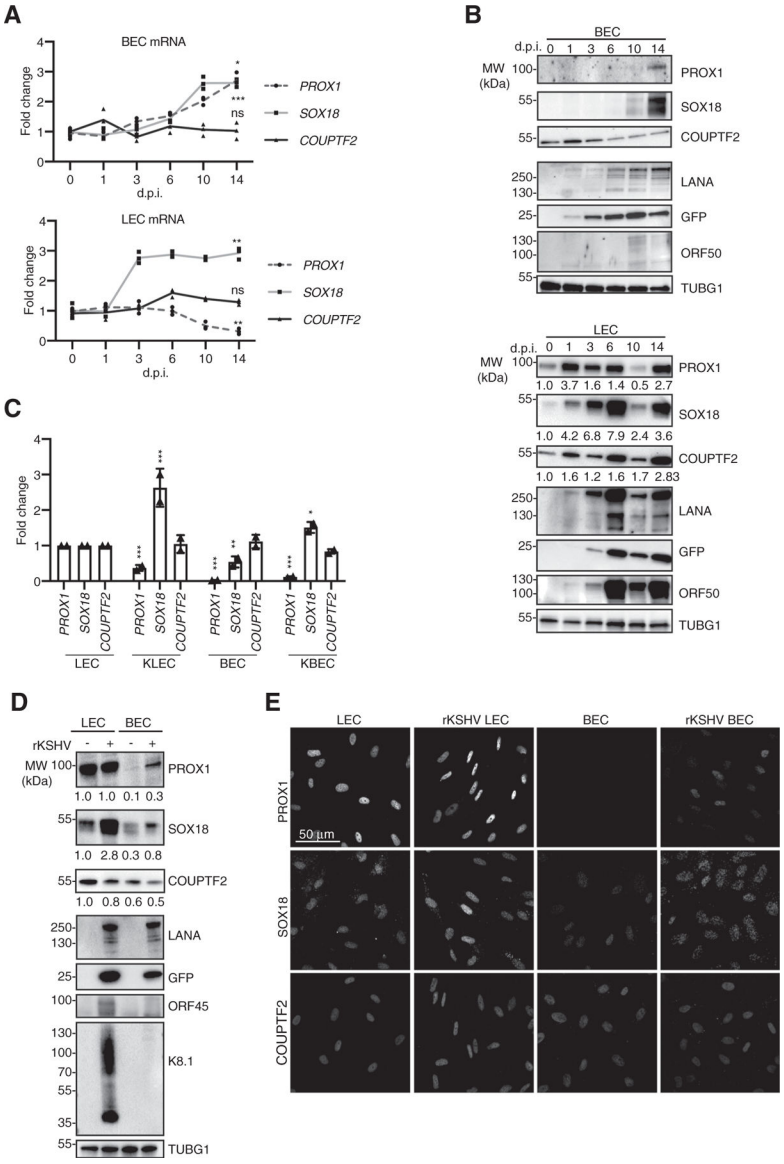

Figure 2.

Endothelial TFs and lytic genes are highly expressed in KLECS. Primary BECs and LECs were infected with rKSHV.219 or left uninfected and analyzed at the indicated timepoints (**A** and **B**) and at 14 d.p.i. (**C–E**). **A,** qRT-PCR for the indicated cellular targets at the indicated timepoint in BECs (top) and LECs (bottom). Single data from $n = 3$ independent experiments ± SD are shown for each timepoint. *P* values were calculated using ordinary one-way ANOVA, followed by Dunnett correction for multiple comparisons. *, $P < 0.033$; **, $P < 0.02$; ***, $P < 0.001$. **B,** Immunoblotting of BECs (top) and LECs (bottom) treated as in **A** for the indicated targets, and γ-tubulin (TUBG1) was used as a loading control. The experiment was repeated three independent times. Numbers below each blot indicate relative band intensity normalized to TUBG1. **C** and **D,** qRT-PCR and immunoblotting, respectively, for the indicated targets at 14 d.p.i., and TUBG1 was used as a loading control. Numbers below each blot indicate relative band intensity normalized to TUBG1.

The experiments were repeated three independent times. **E,** Immunofluorescence staining for PROX1, SOX18, and COUPTF2 in the indicated cell types, treated as in **C** and **D**. Representative images are shown.

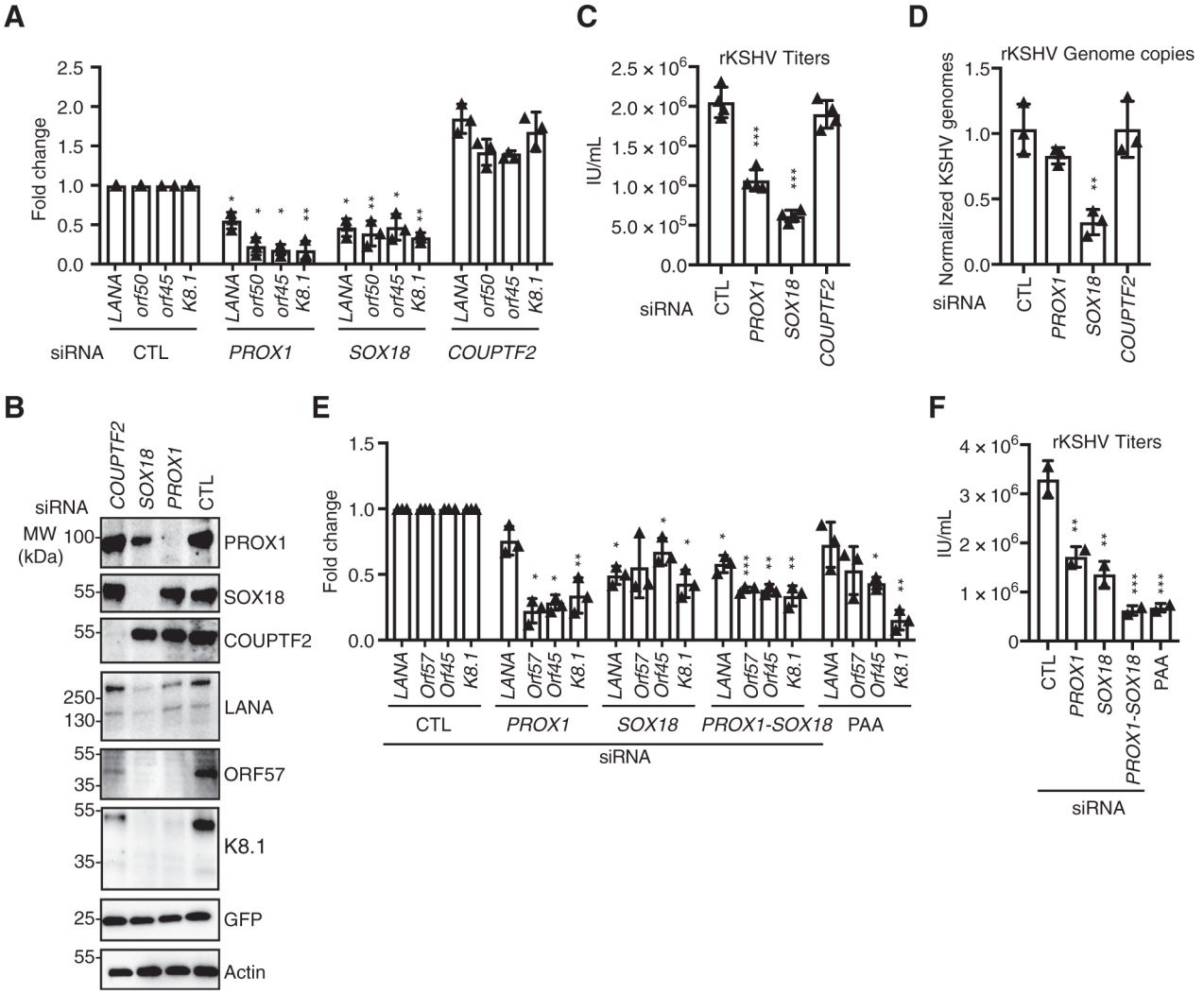

Figure 3.

SOX18 and PROX1 regulate KSHV productive lytic replication cycle through different mechanisms. **A–D,** KLECs were treated at 14 d.p.i. with the indicated siRNAs for 72 hours and analyzed. **A,** qRT-PCR for the indicated targets. Single values from $n = 3$ independent experiments are shown. Bars, mean ± SD. **B,** Immunoblotting for the indicated targets, and actin was used as a loading control. The experiment was repeated three independent times. **C,** Titration of released infectious virus on naïve U2OS cells. Single values from $n = 3$ independent replicates are shown. Bars, mean ± SD. **D,** Relative number of intracellular KSHV genomes. Single values from $n = 3$ independent experiments are shown. Bars, mean ± SD. **E** and **F,** KLECs were treated at 14 d.p.i. with the indicated siRNAs or 0.5 mmol/L PAA for 72 hours. **E,** Cells were analyzed by qRT-PCR for the indicated viral targets. Single values from $n = 3$ independent experiments are shown. Bars, mean ± SD. **F,** Titration of released infectious virus as in **C**. Single values from $n = 2$ independent experiments are shown. Bars, mean ± SD. P values were calculated in **A** and **C–F** using ordinary one-way ANOVA, followed by Dunnett correction for multiple comparisons. *, $P < 0.033$; **, $P < 0.02$; ***, $P < 0.001$.

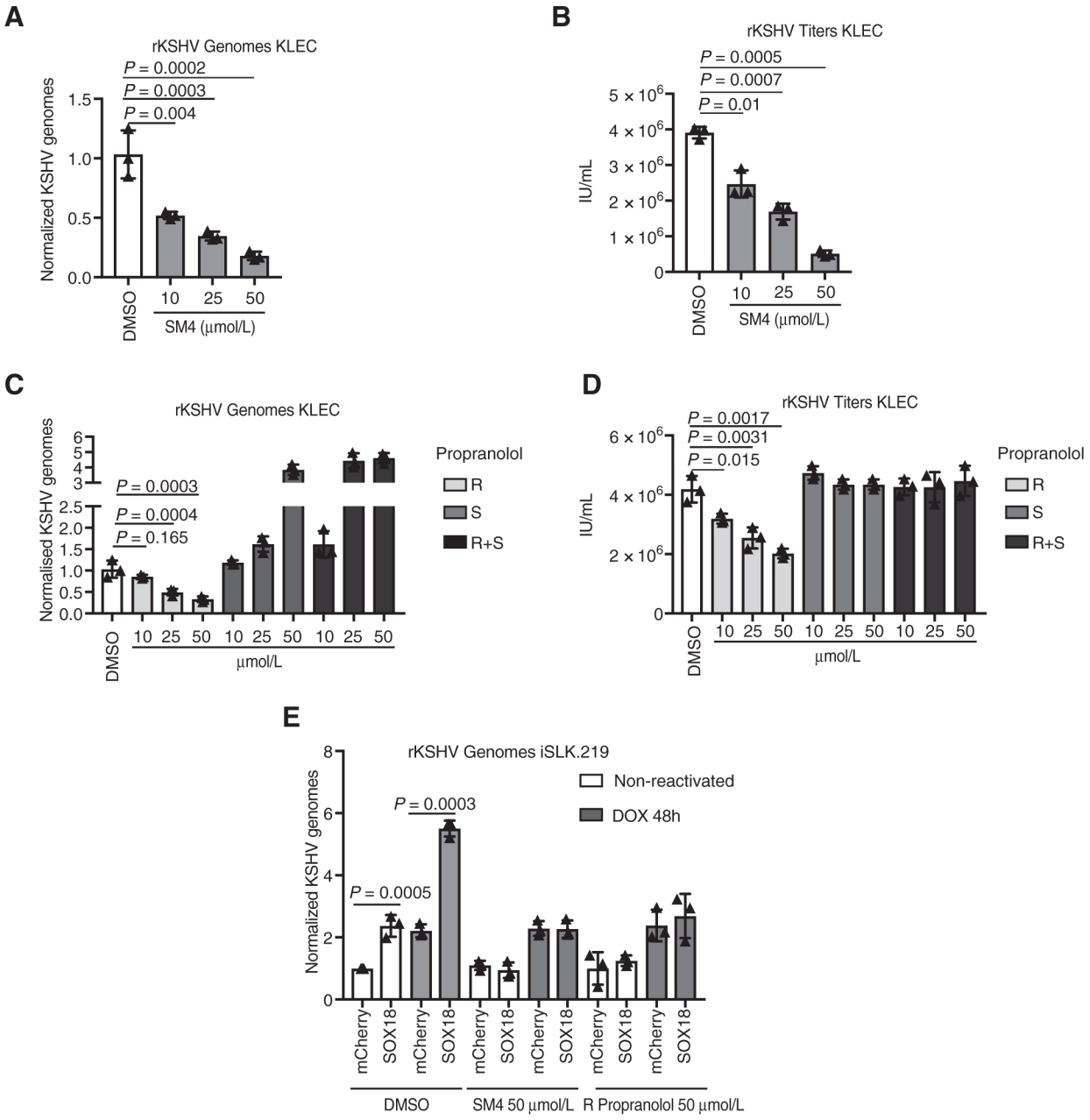

Figure 4.

Selective inhibition of SOX18 efficiently decreases the number of KSHV episome copies. **A–D,** KLECs at 10 d.p.i. were treated with the indicated compounds at the concentrations shown for six days. Every second day, the drug-containing media were refreshed. The relative number of intracellular KSHV genome copies was quantified (**A** and **C**), and the released infectious virus in the supernatant was measured by infecting naïve U2OS cells (**B** and **D**). Single values from $n = 3$ independent replicates are shown. Bars, mean ± SD. *P* values were calculated using ordinary one-way ANOVA, followed by Dunnett correction for multiple comparisons. Exact *P* values are shown. **E,** iSLK.219 cells were transduced with lentiviruses expressing either SOX18 or NLS-mCherry (mCherry) vector control. One day

later, cells were treated either with DMSO or with the indicated drug for 48 hours in the presence or absence of doxycycline for the induction of the lytic cycle. The relative number of intracellular KSHV genome copies was quantified. Single values from $n = 3$ biological experiments are shown. Bars, mean ± SD. *P* values were calculated using two-tailed paired *t* test.

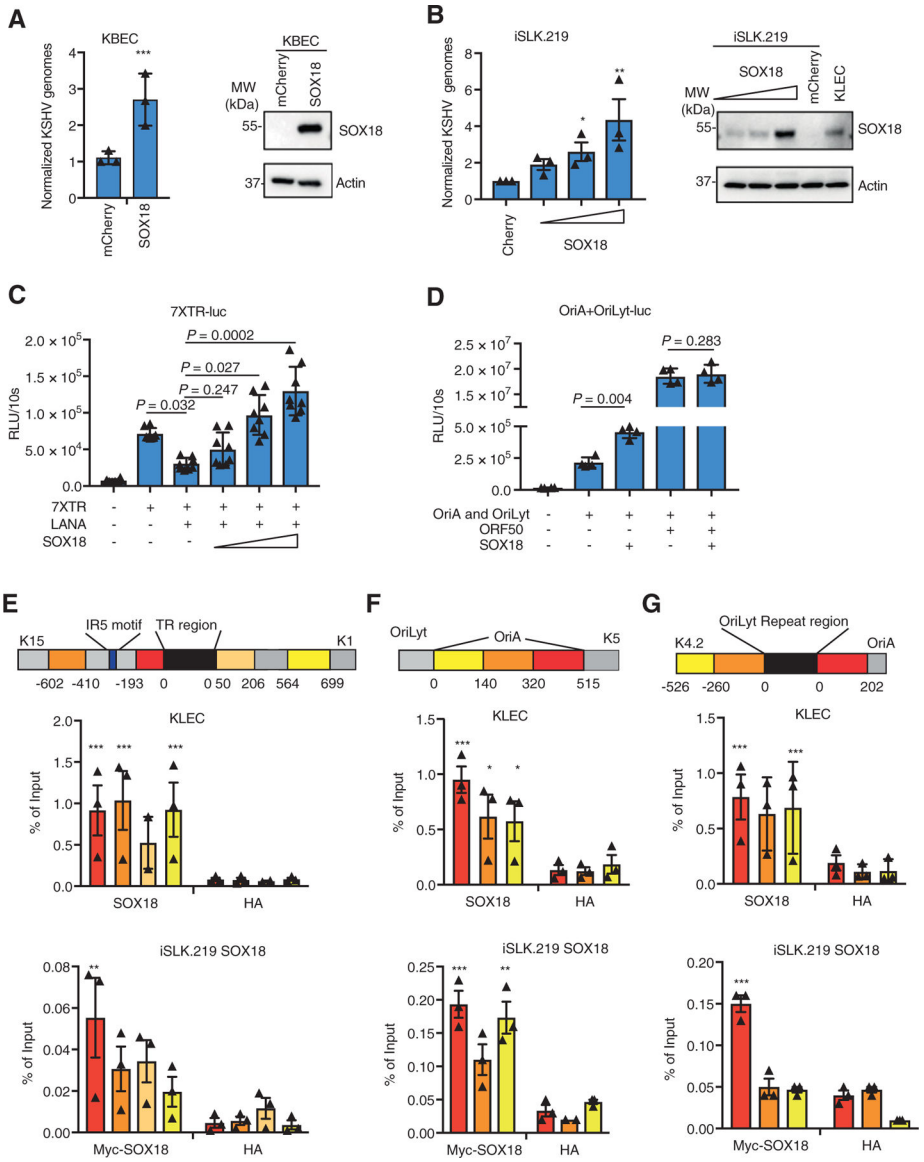

Figure 5.

SOX18 binds to KSHV genome in the proximity of origins of replication. **A** and **B,** Relative number of intracellular KSHV genome copies (left) and immunoblotting for the indicated proteins (right) at 48 hours in KBEC transduced with either SOX18 or NLS-mCherry vector control (mCherry) expressing lentiviruses (**A**) or iSLK.219 cells transduced with increasing doses of lentiviruses expressing either SOX18 or mCherry control (**B**). Single values for n = 3 biological replicates are shown. Bars, mean ± SD. **C** and **D,** Luciferase reporter assays in HeLa cells transfected as indicated. Single values from **C** (n = 8) and D (n = 4) biological replicates are shown. Bars, mean ± SEM. **E–G,** Schematic representation of the promoter regions (top; numbers indicate the nucleotides upstream or downstream of the black regions) amplified by qPCR following ChIP using either anti-SOX18 (middle) or anti-Myc antibodies (bottom) to precipitate endogenous or Myc-tagged SOX18. Anti-HA was used as a negative control. Single values for n = 3 biological replicates are shown. Bars, mean ± SEM. *P*

values in all panels were calculated using ordinary one-way ANOVA, followed by Dunnett correction for multiple comparisons. *, $P < 0.033$; **, $P < 0.02$; ***, $P < 0.001$.

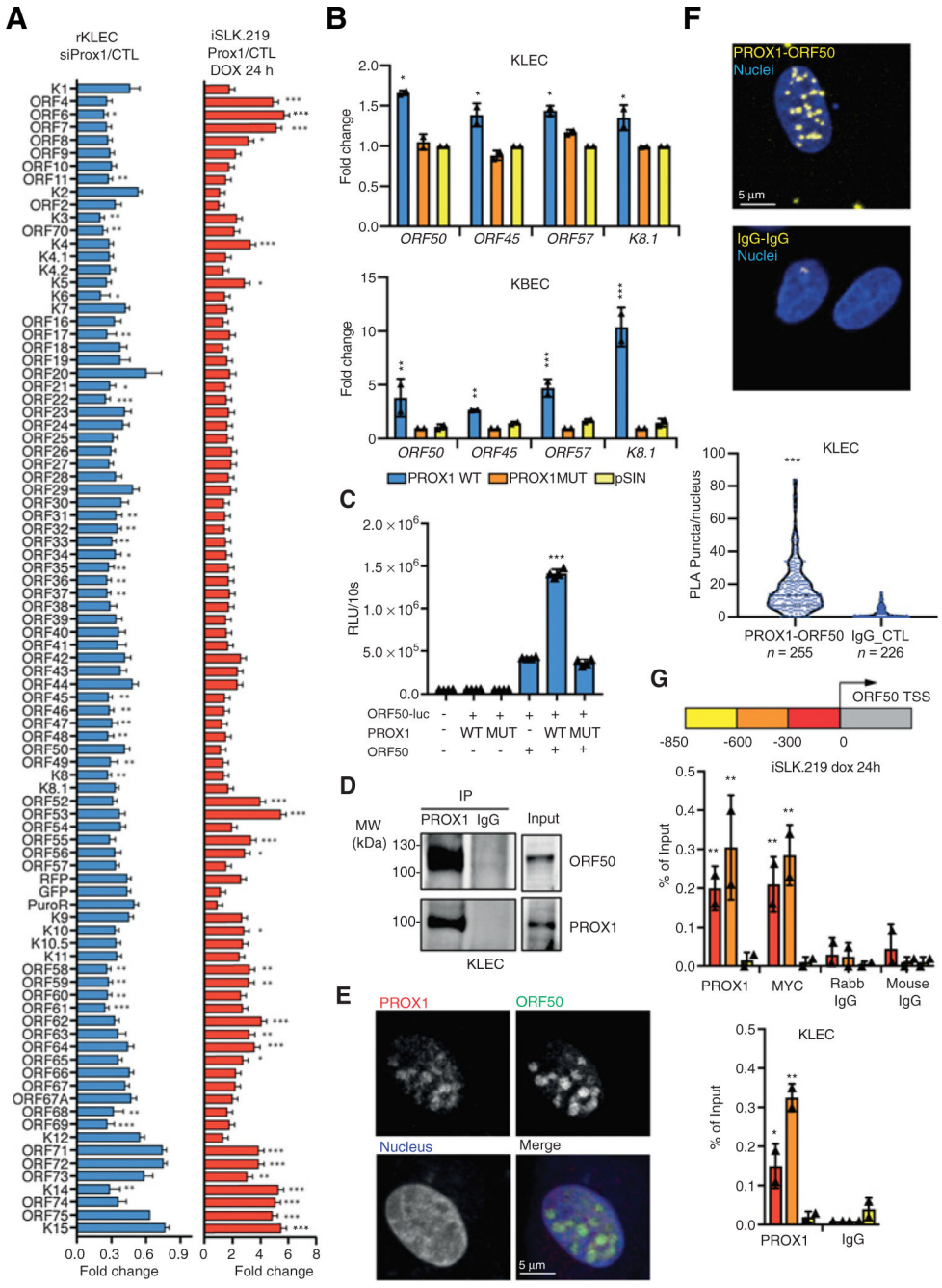

Figure 6.

PROX1 is a positive regulator of viral gene expression, interacts with ORF50, and binds to its promoter region during KSHV lytic replication cycle. **A,** KLECs (left) and iSLK.219 cells (right) in $n = 3$ independent replicates were treated as indicated and subjected to RNA-seq. Fold change ± SEM in the viral transcripts over the appropriate control is shown. **B,** KLECs (top) and KBECs (bottom) were transduced with the indicated lentiviral vectors for 72 hours. Cells were analyzed by qRT-PCR for the indicated targets. Single values from $n = 2$ independent experiments are shown. Bars, mean ± SD. **C,** Luciferase reporter assay in HEK293FT transfected with the indicated plasmids for 36 hours. Single values

for $n = 4$ biological replicates are shown. Bars, mean ± SD. **D,** Coimmunoprecipitation of PROX1 with ORF50 in KLECs. The experiment was repeated two independent times. **E,** Immunofluorescence for PROX1 (red) and ORF50 (green) in KLECs infected with WT KSHV at 16 d.p.i. A representative image is shown; the experiment was done two times. **F,** PLA with antibodies against PROX1 and ORF50, or IgG control. Top and middle, PLA signal is shown by yellow puncta. Nuclei were counterstained with Hoechst 33342. Bottom, quantification of PLA puncta/nucleus; *n*, number of nuclei quantified. The experiment was repeated two independent times. **G,** Top, schematic representation of the *ORF50* promoter regions (numbers indicate the nucleotides upstream of the *ORF50* TSS) amplified by qPCR following ChIP. Middle, ChIP in iSLK.219 cells transduced with lentivirus expressing Myc-tagged PROX1 reactivated (doxycycline) for 24 hours. ChIP was performed with anti-PROX1 and anti-Myc and DNA was amplified in the promoter regions of the *ORF50* gene. Bottom, ChIP in KLECs 14 d.p.i. using anti-PROX1 antibody as above. Bars, mean ± SD. *P* values in **A–C, F,** and **G** were calculated using ordinary one-way ANOVA, followed by Dunnett correction for multiple comparisons. *, $P < 0.033$; **, $P < 0.02$; ***, $P < 0.001$.

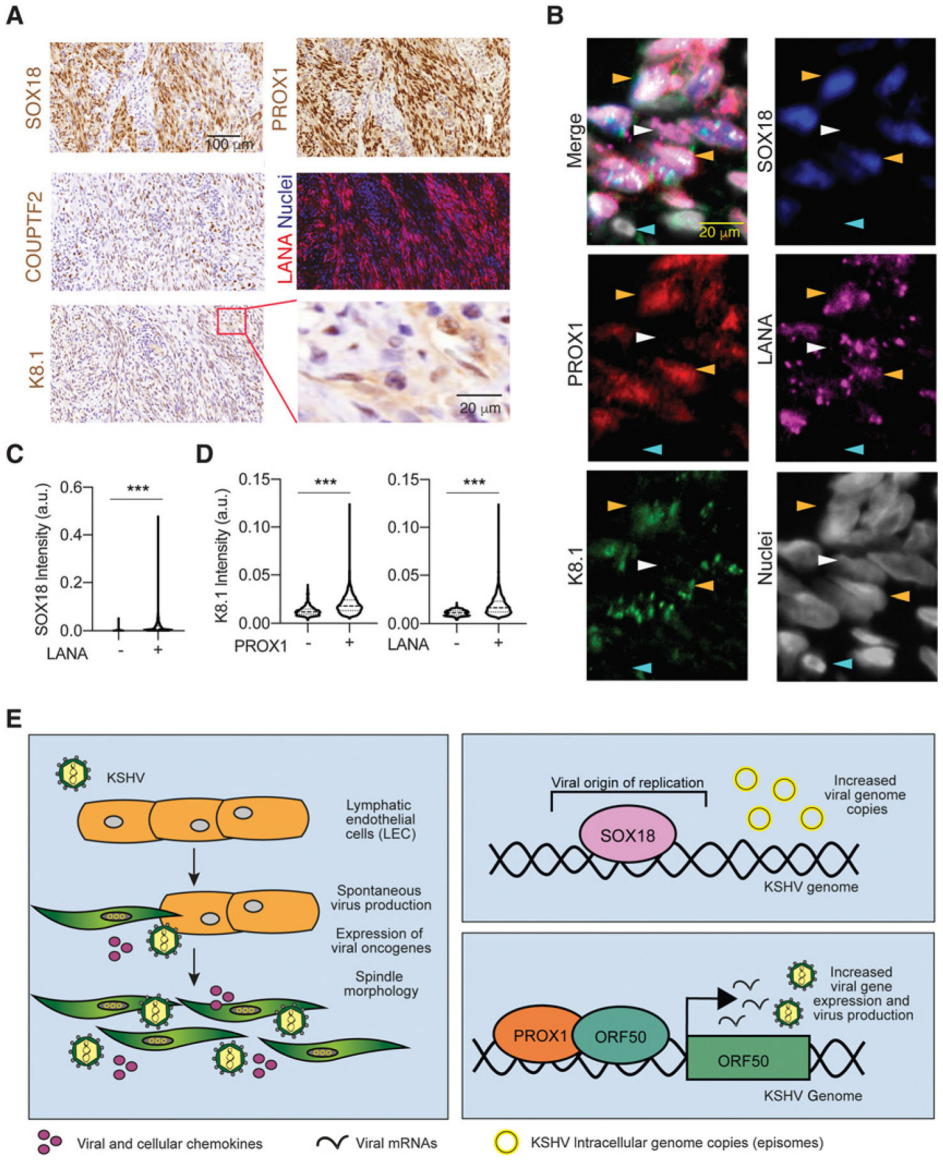

Figure 7.

PROX1, SOX18, COUPTF2, and K8.1 are expressed in Kaposi sarcoma tumors. **A,** Representative images of consecutive sections from AIDS-Kaposi sarcoma biopsy stained as indicated. The red box indicates the portion of the biopsy magnified in the right inset. **B–D,** Multiplex IHC staining of 19 Kaposi sarcoma biopsies for PROX1, SOX18, LANA, and K8.1. Correlation was calculated considering the mean intensity of each staining for 8345 tumor cells across the 19 biopsies (mean: 439 cells/biopsy; range: from 102 to 754 cells/biopsy analyzed). K8.1 versus LANA: Pearson correlation coefficient (PCC):0.181, $P < 0.0001$; K8.1 versus PROX1: PCC:0.407, $P < 0.0001$; LANA versus PROX1: PCC:0.626, $P < 0.0001$; LANA versus SOX18: PCC:0.434, $P < 0.0001$. K8.1 versus SOX18: PCC:0.148, $P < 0.0001$. P values were corrected for the false discovey rate using the Bonferroni correction. **B,** Representative image. Nuclei were counterstained with DAPI. Orange arrowheads, cells positive for all the markers; white arrowhead, a cell positive for LANA but not for the other

markers; cyan arrowhead, uninfected cells. **C** and **D,** Violin plots showing marker intensities with continuous values (*y*-axis) and categorized values for cells negative (−) or positive (+) for the indicated marker (*x*-axis). For the categorized LANA and PROX1, the lowest quartile intensities were set as the negativity/positivity thresholds, equaling to 2.7-fold and 2.6-fold background intensities (minimum cell value), respectively. a.u., arbitrary units. ***, $P < 0.0001$. **E,** Schematic model of the role of KSHV spontaneous lytic replication in the expansion of viral infection in a LEC culture (left) and of the roles of SOX18 (top right) and PROX1 (bottom right) as positive regulators of viral episome copy numbers, lytic gene expression, and infectious virus release, respectively.